

Recent Advances in Polarized He-3 Targets

Jaideep Singh^{1*}, Peter Dolph*, Karen Mooney*, Vladimir Nelyubin*,
Al Tobias*, Aidan Kelleher[†], Todd Averett[†] and Gordon Cates*

**Physics Department, University of Virginia, P.O.Box 400714, Charlottesville, VA 22904-4714*

[†]*Dept. of Physics, The College of William & Mary, P.O. Box 8795, Williamsburg, VA 23187-8795*

Abstract. Recently there have been many important advances made in spin-exchange optical-pumping (SEOP) polarized He-3 targets. Use of hybrid K-Rb SEOP achieved He-3 polarizations near 50% in-beam during the recent JLab G_E^n experiment (E02013). Combining well-optimized alkali-hybrid SEOP with high-power spectrally-narrowed laser diode arrays increases He-3 polarizations to 70%. We describe how these technologies work and why they improve target polarization.

Keywords: laser-polarized helium-3 targets for electron scattering, alkali-hybrid spin-exchange optical pumping, spectrally-narrowed laser diode arrays, hybrid potassium-rubidium (K-Rb) SEOP

PACS: 29.25.Pj,67.30.ep,32.80.Xx,25.30.c

INTRODUCTION

The focus of this talk are high-density two-chamber SLAC/JLab-style spin-exchange optical-pumping (SEOP) polarized ^3He target cells. Over the last 20 years, they have been used to make precise measurements of the neutron electromagnetic form factors G_E^n & G_M^n , spin asymmetry A_1^n , and spin structure functions g_1^n & g_2^n . The first SLAC-type cells were expected to achieve 50% [1], whereas the average polarization in-beam during the SLAC experiments (E142 & E154) was more typically 35% [2, 3]. Until recently, the performance of the JLab cells had been marginally better ($\approx 40\%$) and the ^3He polarization rarely exceeded 50%. The use of alkali-hybrid SEOP alone has consistently increased the ^3He polarization over 50%. In combination with high-power spectrally-narrowed (narrowband) laser diode arrays, the ^3He polarization now regularly approaches 70%. The purpose of this talk is to demonstrate how to optimize ^3He polarization using alkali-hybrid SEOP & narrowband lasers.

TRADITIONAL SPIN-EXCHANGE OPTICAL PUMPING

In traditional SEOP, a single alkali species, in our case rubidium (Rb), (1) is polarized by optical pumping and then (2) transfers its electronic polarization to the ^3He nuclei by spin-exchange collisions. Optical pumping occurs by exciting the D1 transition of the Rb vapor (795 nm) by circularly polarized laser light. If the light propagates along the axis of the applied magnetic field, then (ignoring the Rb nuclear spin) only one of the two Zeeman levels ($m_J = \pm 1/2$) of the $5S_{1/2}$ ground state is selectively excited to

¹ corresponding author, email: js7uq@virginia.edu

the $5P_{1/2}$ state. Because the levels of the excited states are mixed due to collisions, the Rb atom can decay back to either Zeeman level of the ground state with equal probability. Decays dominated by radiation would limit the optical-pumping efficiency; therefore, just enough N_2 is added to nonradiatively quench the $5P_{1/2} \rightarrow 5S_{1/2}$ transition. On a timescale of milliseconds, the Rb polarization reaches an equilibrium value of $P_{\text{Rb}} = 1 / (1 + \Gamma_{\text{Rb}}/R)$, where the optical-pumping rate is given by:

$$R = \int_0 \phi(\nu) \cdot \sigma(\nu) d\nu \approx 115 \text{ kHz per } 75 \text{ W}/23 \text{ cm}^2/2 \text{ nm (broadband limit)} \quad (1)$$

where $\phi(\nu)$ is the photon flux and $\sigma(\nu)$ is the Rb D1 photon-absorption cross section (which is a δ -function in the broadband limit). The Rb spin-relaxation rate is given by:

$$\Gamma_{\text{Rb}} = k_{\text{Rb}}[\text{Rb}] + k_{\text{He}}[{}^3\text{He}]_{\text{pc}} + k_{\text{N}_2}[\text{N}_2]_{\text{pc}} \approx 1 \text{ kHz} \quad (200^\circ\text{C} \ \& \ [{}^3\text{He}]_{\text{pc}} = 7 \text{ amg}) \quad (2)$$

where k_X is the Rb spin-relaxation rate constant for Rb-X collisions and $[X]$ refers to the X number density. The main source of this relaxation is a spin-orbit coupling between the Rb valence electron and the orbital angular momentum of the Rb-X pair. This is analogous to the spin-orbit coupling that occurs within an alkali atom A; therefore, the strength of the A-X spin-orbit coupling scales with the A spin-orbit splitting [4].

A hyperfine-like Fermi-contact interaction couples the valence electron spin of the Rb atom to the nucleus of the ${}^3\text{He}$ atom. The small but nonzero probability that spin exchange occurs between the Rb electron and the ${}^3\text{He}$ nuclear spin is quantified by the Rb- ${}^3\text{He}$ spin-exchange rate constant ($k_{\text{se}} = 10^{-15} \text{ cm}^3/4.08 \text{ hrs}$ [5]). In the SLAC/JLab design, optical pumping and spin exchange occur only in the spherical pumping chamber (6–9 cm diameter, $[{}^3\text{He}]_{\text{pc}} = 7 \text{ amg}$). The polarized ${}^3\text{He}$ nuclei subsequently diffuse through a transfer tube to the cylindrical target chamber (15–40 cm long, $[{}^3\text{He}]_{\text{tc}} = 10 \text{ amg}$), where the electron scattering occurs. The pumping chamber is heated to insure an adequate Rb vapor pressure. On a timescale of several hours, the ${}^3\text{He}$ polarization (in the fast diffusion limit) reaches an equilibrium value of $P_{\text{He}} = P_{\text{Rb}} / (1 + \langle\Gamma_{\text{He}}\rangle / \langle\gamma_{\text{se}}\rangle)$ where $\langle\Gamma_{\text{He}}\rangle = f_{\text{pc}}\Gamma_{\text{pc}} + f_{\text{tc}}\Gamma_{\text{tc}}$ is the cell-averaged ${}^3\text{He}$ spin-relaxation rate, $\langle\gamma_{\text{se}}\rangle = f_{\text{pc}}k_{\text{se}}[\text{Rb}]$ is the cell-averaged spin-exchange rate, $f_{\text{pc(tc)}}$ (≈ 0.5 for our cells) is the fraction of nuclei in the pumping (target) chamber, and $\Gamma_{\text{pc(tc)}}$ the ${}^3\text{He}$ spin-relaxation rate in the pumping (target) chamber.

Using nothing more than Eqns. (1) & (2), we find $P_{\text{Rb}} \geq 99\%$. Combining this with typical values for $\langle\Gamma_{\text{He}}\rangle = 0.02/\text{hrs}$ & $\langle\gamma_{\text{se}}\rangle = 0.1/\text{hrs}$, we obtain $P_{\text{He}} = 83\%$. There are two reasons why this naive estimate is double what we regularly obtain with traditional SEOP using broadband lasers. First, it has been reported that there is a ${}^3\text{He}$ spin-relaxation mechanism, the X-factor, that appears to scale with the alkali density [6]. Second, the estimate for P_{Rb} is woefully inadequate because it doesn't account for the spatial variation of the photon flux due to the light absorption by Rb:

$$\partial\phi(\vec{r}, \nu)/\partial z = -\phi(\vec{r}, \nu)\sigma(\nu)[\text{Rb}](1 - P_{\text{Rb}}(\vec{r})) \quad (3)$$

where z is the depth into the cell and $[\text{Rb}] \approx 10^{15}/\text{cm}^3$. Because the Rb polarization rate (kHz) is much faster than its diffusion rate (mHz), the *local* Rb polarization is given by the *local* optical-pumping rate, which in turn depends on the *local* photon flux. On

the other hand, because the ^3He diffusion rate (mHz) is much faster than its polarization rate (μHz), the ^3He polarization actually depends on the average Rb polarization in the pumping chamber ($\langle P_{\text{Rb}} \rangle_{\text{pc}}$). Thus the ^3He equilibrium polarization is more accurately given by $P_{\text{He}} = \langle P_{\text{Rb}} \rangle_{\text{pc}} / (1 + X + \langle \Gamma_{\text{He}} \rangle / \langle \gamma_{\text{se}} \rangle)$. We'll now focus on the shape of the Rb polarization gradient, which depends crucially on the spectral width of the laser.

SPECTRALLY-NARROWED LASER DIODE ARRAYS

The spectral profile of the type of laser diode arrays used for optical pumping can be represented by a gaussian line shape with a characteristic width given by the full width at half maximum $\Delta\nu$. The relevant scale with which to compare $\Delta\nu$ is the pressure-broadened Rb D1 absorption line width ($\Gamma_1 \approx [^3\text{He}]_{\text{pc}} \cdot 0.04 \text{ nm}/\text{amg} = 0.3 \text{ nm}$). For the last 10 yrs, we've used up to five 30 Watt Coherent FAP systems [7] with spectral widths of $\Delta\nu \approx 2 \text{ nm}$. This is relatively broad and is a direct consequence of the naturally broad gain profile of the laser diode bars. Recently, we've performed tests with up to three 25 Watt Spectra-Physics Comets [8]. These lasers have volume Bragg gratings (VBG) coupled directly to the output of the laser diode bars. A narrow slice of the gain profile is amplified by reflecting wavelength-selected light by the VBG back into the laser diode bar. This "narrows" the spectral width to $\Delta\nu \approx 0.2 \text{ nm}$ for $\approx 90\%$ of the power.

The first advantage of these narrowband lasers is the dramatic factor of ≈ 5 increase in the optical-pumping rate for the same laser power [9]. The second advantage is the shape of the Rb polarization gradient that the light creates along its propagation path, see Fig. 1. At the front of the pumping chamber, the resonant part of the laser spectrum dominates the optical pumping and produces near unity Rb polarization. However, even at very high Rb polarization, a small amount of light is absorbed, mainly from the resonant part of the laser spectrum. After a sufficiently large distance, the resonant part of the laser spectrum is completely absorbed. At this depth, for a broadband laser, the off-resonant part of the laser spectrum continues to polarize the Rb, but at a much lower level. Consequently, the light penetrates further and the Rb polarization gradually rolls off to zero. On the other hand, for a narrowband laser, the *entire* spectrum is resonant. Therefore, once the Rb polarization starts to drop, the light is even more strongly absorbed and the Rb polarization drops sharply to zero.

If this sharp drop occurs well before the back end of the cell, then the Rb polarization averaged over the path is roughly the same for broadband and narrowband lasers with the same power. Therefore, to fully take advantage of narrowband lasers, the depth at which this sharp drop occurs must be located past the back end of the pumping chamber. Under this condition, the Rb polarization is near unity along the entire light path. We can accomplish this by lowering $[\text{Rb}]$ and/or increasing the laser power.

ALKALI-HYBRID SPIN-EXCHANGE OPTICAL PUMPING

In alkali-hybrid SEOP [10, 11], a mix of two alkali species, in our case potassium (K) & rubidium (Rb), are used. As before, Rb is polarized by optical pumping. When the K to Rb vapor density ratio ($D = [\text{K}]/[\text{Rb}]$) is small ($D \ll 1000$), extremely efficient K-Rb

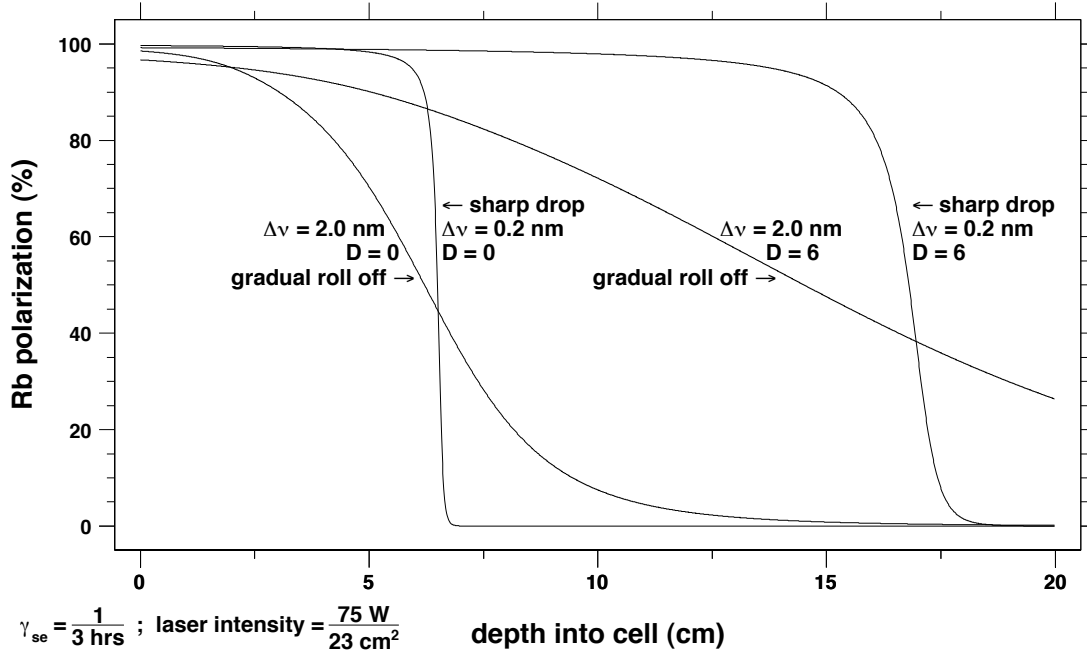


FIGURE 1. (NUMERICAL SIMULATION) Rb polarization gradient for fixed γ_{se} & laser intensity. Traditional (hybrid K-Rb) SEOP is depicted by the two curves labeled $D = 0$ ($D = 6$) on the left (right). Note the difference in shape between broadband ($\Delta\nu = 2$ nm) & narrowband ($\Delta\nu = 0.2$ nm) lasers.

spin-exchange collisions insure that $P_K = P_{Rb} = P_A$. Now both K & Rb polarize ^3He by spin-exchange collisions. The equations for the equilibrium polarizations have the same form provided we relabel the subscript Rb \rightarrow A and account for the spin relaxation & exchange due to K:

$$\Gamma_A = \Gamma_{Rb} + D(\Gamma_K + 2k_A[\text{Rb}]) \quad \& \quad \langle \gamma_{se} \rangle = f_{pc} k_{se} [\text{Rb}] (1 + D \cdot k'_{se} / k_{se}) \quad (4)$$

where $\Gamma_K \approx 0.2$ kHz (235°C & $[^3\text{He}]_{pc} = 7$ amg) is the K spin-relaxation rate, k_A is the mean K-Rb spin-relaxation rate constant, and $k'_{se} = 10^{-15}$ cm³/5.05 hrs [12] is the K- ^3He spin-exchange rate constant. Since K has a much smaller spin-orbit splitting than Rb (3.5 nm vs. 15 nm), K also has a much smaller spin-relaxation rate than Rb.

Following the closing argument of the previous section, let's lower $[\text{Rb}]$ while keeping the laser power fixed. In traditional SEOP ($D = 0$), lowering $[\text{Rb}]$ has the undesirable effect of also lowering $\langle \gamma_{se} \rangle$. On the other hand, in hybrid K-Rb SEOP ($D > 0$), we can lower $[\text{Rb}]$ while keeping $\langle \gamma_{se} \rangle$ fixed, provided we increase D by the correct amount. *If the increase in Γ_A (due to the increase in D) is not too large*, then the light would penetrate farther into the pumping chamber for the hybrid case (because K absorbs very little light near the Rb D1 wavelength). Consequently, for a narrowband laser, the sharp drop in Rb polarization would occur even farther away from the front of the pumping chamber, see Fig. 1. To achieve the best balance between Γ_A and $\langle \gamma_{se} \rangle$, the optimal range for D must be found.

EXPERIMENTAL RESULTS & CONCLUSIONS

To make a cell that will have a prescribed ratio (D_{goal}) when the pumping chamber is hot, we must prepare a mix of solid alkali metal with the correct mole fractions of Rb & K (f_{Rb} & f_{K}). According to Raoult's law, the partial vapor pressure due to one constituent of an ideal solution is given by the product of that constituent's mole fraction and pure vapor pressure. A solution of K & Rb is nearly ideal because chemical interactions between K & K, Rb & Rb, and K & Rb are all similar. Consequently Raoult's law is satisfied very well and, combining it with the pure vapor pressure curves for K & Rb [13], gives the ratio of mole fractions

$$\frac{f_{\text{Rb}}}{f_{\text{K}}} \approx \frac{1}{6.31 \cdot D_{\text{goal}}} \times \left(\frac{[\text{K}]_{\text{goal}}}{10^{14} \text{ cm}^{-3}} \right)^{0.097} \quad (\text{valid for } D_{\text{goal}} \gg 0.2) \quad (5)$$

necessary to obtain D_{goal} at the oven temperature where the desired K density is $[\text{K}]_{\text{goal}}$. Using a glove box, we've found that we can prepare a break-seal ampoule with the desired $f_{\text{Rb}}/f_{\text{K}}$ to better than 15%. However, transferring the alkali mix from the ampoule into the pumping chamber introduces variations. For every cell that we've measured the ratio under operating conditions (D_{meas}), our preliminary analysis has shown $D_{\text{meas}} \leq 1.2 \cdot D_{\text{goal}}$. In addition, we've found for cells with $D_{\text{goal}} = 20$ that $D_{\text{meas}} = 9.2 \pm 6.4$ and for cells with $D_{\text{goal}} = 5$ that $D_{\text{meas}} = 3.0 \pm 1.6$. Fig. 2 depicts the highest ^3He polarization achieved as a function of D with both broadband and narrowband lasers. Because these data were taken over several years with different cells, the laser conditions and the intrinsic ^3He spin-relaxation rates vary as well. With that caveat, we still feel that we can make the following preliminary claims: (1) the ideal vapor density ratio under our typical operating conditions is $2 \leq D \leq 6$, (2) even replacing a single broadband laser with a narrowband laser produces significant gains, (3) to achieve near 70% ^3He polarization in the pumping chamber, one needs to use both hybrid K-Rb SEOP and narrowband lasers and (4) because P_{He} is so high now, a magnetic field gradient ($\approx 10 \text{ mG/cm}$) must be applied to prevent masing [3].

The variation in D_{meas} from D_{goal} almost perfectly overlaps the observed optimal range for D provided $D_{\text{goal}} = 5$. In other words, the level of control that we have over D for a given cell is sufficient to fall within the optimal range for D . Since we don't have arbitrary control over the spectral width of the laser, we've run several numerical simulations. Generally speaking, we've found that a spectral width that is roughly equal to the absorption line width is sufficiently narrow to obtain the significant benefits of optical pumping with narrowband lasers. Analysis is underway to calculate the X -factors for our cells by combining measurements of the alkali & ^3He polarizations, the alkali densities, and the ^3He polarization build-up & decay rates. The extraction of X is complicated by the polarization diffusion between the pumping & target chambers.

In conclusion, spectrally-narrowed lasers are most effective when the depth at which the sharp drop in Rb polarization occurs is beyond the back end of the pumping chamber. Because both the depth of this sharp drop & the back end of the pumping chamber vary with the radial distance from the propagation axis, care must be taken to match the laser beam size to the pumping chamber. In that case, the entire pumping chamber is illuminated and the average Rb polarization is nearly unity. Alkali-hybrid SEOP is

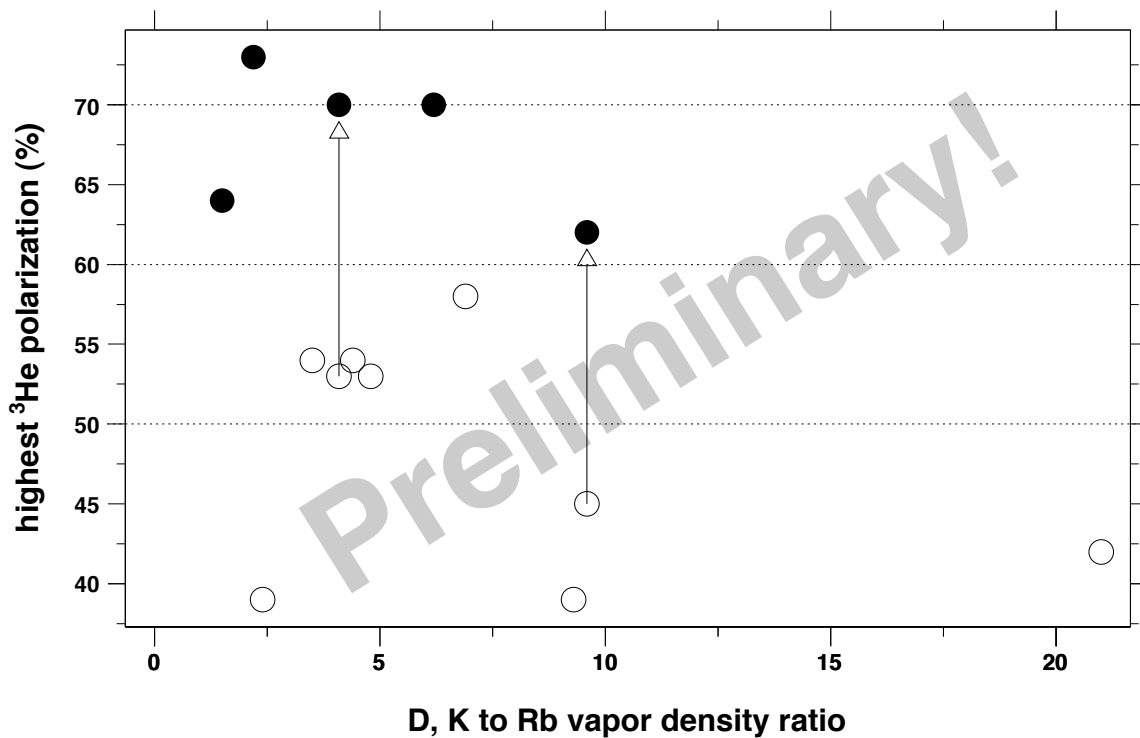


FIGURE 2. (PRELIMINARY DATA) Highest ³He polarization achieved as a function of D using broadband (open circles) & narrowband (closed circles) lasers. The arrows indicate the increase in polarization for the same cell when the lasers are switched from broadband to narrowband.

effective because it partially decouples the photon cost from a high spin-exchange rate. Finally, we infer from measurements of the alkali polarization & the analysis presented in this talk that traditional SEOP with broadband lasers failed to achieve our naive expectations, at least in part, due to unexpectedly low *average* Rb polarization ($\langle P_{\text{Rb}} \rangle_{\text{pc}}$).

REFERENCES

1. E.W. Hughes, et al., *SLAC E-142 Proposal*, 1989.
2. H. L. Middleton, Ph.D. thesis, Princeton University (1994).
3. M. V. Romalis, Ph.D. thesis, Princeton University (1997).
4. T. G. Walker, J. H. Thywissen, and W. Happer, *Phys. Rev. A* **56**, 2090–2094 (1997).
5. A. Ben-Amar Baranga, et al., *Phys. Rev. Lett.* **80**, 2801–2804 (1998).
6. E. Babcock, et al., *Phys. Rev. Lett.* **96**, 083003 (2006).
7. FAPSys-Rubidium-30W-795to798-Single, Coherent, Inc., 5100 Patrick Henry Drive, Santa Clara, CA USA 95054, 800-527-3786.
8. VBG locked Comet, 30W, 794.7 nm, 400 μm core fiber, Spectra-Physics (a division of Newport Corporation), 3321 E. Global Loop, Tucson, AZ USA 85706, 520-746-1234.
9. B. Chann, et al., *J. Appl. Phys.* **94**, 6908–6914 (2003).
10. W. Happer, G. D. Cates, Jr., M. V. Romalis, and C. J. Erickson, *U.S. Patent No. 6,318,092* (2001).
11. E. Babcock, et al., *Phys. Rev. Lett.* **91**, 123003 (2003).
12. E. V. Babcock, Ph.D. thesis, University of Wisconsin-Madison (2005).
13. *CRC Handbook of Chemistry and Physics*, CRC Press, Boca Raton, FL, 1994, 75th student edn.